Electrochemistry of the copper–nickel series of heteropolymetallic complexes [(μ_4-O){NC$_5$H$_4$[C(O)NEt$_2$]-3}$_4$Cu$_{4-x}${Ni(H$_2$O)}$_x$Cl$_6$] (x = 0–4)†
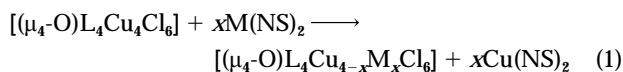
Bizuneh Workie,[a] Christopher E. Dubé,[a] Levent Aksu,[a] Samuel P. Kounaves,*,[a] Albert Robbat, Jr.[a] and Geoffrey Davies[b]

[a] Department of Chemistry, Tufts University, Medford, MA 02155, USA
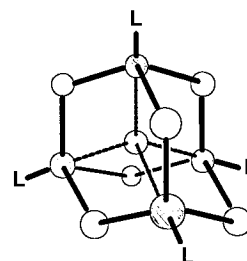[b] Department of Chemistry, Northeastern University, Boston, MA 02115, USA

The electrochemistry of the tetranuclear copper–nickel heteropolymetallic complexes [(μ_4-O)L$_4$Cu$_{4-x}${Ni-(H$_2$O)}$_x$Cl$_6$] [x = 0–4, L = N,N-diethylnicotinamide (denc)] were studied at a platinum electrode in dimethyl sulfoxide with 0.20 M tetrabutylammonium hexafluorophosphate as supporting electrolyte. At potentials more cathodic than -1.0 V the complexes are electrodeposited as Cu–Ni alloy and metal oxide films and display a complicated set of cyclic voltammographs. The voltammographs of all the Cu-containing complexes show a quasi-reversible redox couple in the potential range 0.250 to -0.450 V *vs.* Ag–AgPF$_6$ (0.01 M)–CH$_3$CN. As the number of Cu atoms decreases in the complex, the peak currents i_{pa} and i_{pc} decrease proportionally and the peak potential shifts anodically. The cyclovoltammetric (CV) results indicate that electron transfer initially occurs only to the Cu^{II} centres and that the electron-transfer reaction appears to be quasi-reversible. Using steady-state voltammetry at an ultramicroelectrode in combination with chronoamperometry at a microelectrode and exhaustive electrolysis at a Hg-pool electrode, the number of electrons (n) transferred for this initial reduction of the Cu$_4$, Cu$_3$Ni, Cu$_2$Ni$_2$ and CuNi$_3$ complexes were 3.1, 2.1, 1.8 and 0.57, respectively. The diffusion coefficient for all the complexes was $2.2(\pm0.1) \times 10^{-6}$ cm^2 s^{-1}. The electronic spectrum of the Cu$_4$ complex taken after exhaustive electrolysis shows that one quarter of the Cu atoms remain in the Cu^{II} form and that the Cu^I complex remains stable. Since only a single CV peak results for all of the complexes, the electron transfer is most likely consecutive with very closely spaced E° potentials. A model based on statistically determined electron transfer to Cu^{II} in particular faces is also proposed.

The tetranuclear copper(II) complexes [(μ_4-O)L$_4$Cu$_4$Cl$_6$] with L typically being a pyridine derivative, have been reported in the literature since the mid 1960s.[1-3] Their structures,[2,4-7] spectrochemical,[8-11] thermal,[12] and magnetic[8,9] behaviours have been subjected to extensive investigation. Structurally, these complexes are adamantane-like, with four Cu^{II} centres of distorted trigonal-bipyramidal geometry bridged in pairs by Cl atoms, a central tetrahedral oxygen and one organic ligand co-ordinated to each copper. Davies and co-workers[13-18] found that these complexes have Cu atoms that can be successively and stoichiometrically replaced with other metal atoms without altering the overall geometry. This process, known as transmetallation, is accomplished using reagents called transmetallators and can be used to give families of heteropolymetallic (HPM) products as given by equation (1). In this equation NS is

$$[(\mu_4\text{-O})\text{L}_4\text{Cu}_4\text{Cl}_6] + x\text{M(NS)}_2 \longrightarrow$$
$$[(\mu_4\text{-O})\text{L}_4\text{Cu}_{4-x}\text{M}_x\text{Cl}_6] + x\text{Cu(NS)}_2 \quad (1)$$

S-methyl isopropylidenehydrazinecarbodithioate, L is a nitrogen-donor ligand such as monodentate N,N-diethylnicotinamide (denc) or pyridine (py), and M is a metal such as Ni, Co or Zn. The transmetallation phenomenon and its requirements, patterns and products have been well established.[13-15]

Previous electrochemical studies of [(μ_4-O)L$_4$Cu$_{4-x}${Ni-(H$_2$O)}$_x$Cl$_6$] (x = 0–4, L = denc or py) had suggested that these complexes are electrochemically inactive.[19] The only reported exception to this finding was for the related complexes [(μ_2-Y)-L$_4$Cu$_{4-x}$(OH)$_2$Ni$_x$Cl$_4$]·3H$_2$O (x = 0–4, Y = 3,4,5,6-tetrachlorocatecholate) which exhibited 'quasi-reversible' cyclic voltammetric behaviour with the peak potentials altered by the substi-

tution of nickel for copper.[19] However, the results are not directly applicable to the large family of [(μ_4-O)L$_4$Cu$_{4-x}$M$_x$Cl$_6$] complexes because of the structural differences and the lack of the highly electroactive catecholate group.

Recent work in our laboratory[20-22] has shown that, in addition to being electroactive, the series of [(μ_4-O)(denc)$_4$(Cu$_{4-x}$-{Ni(H$_2$O)}$_x$Cl$_6$] complexes with x = 0–4 when dissolved in dimethyl sulfoxide (dmso) with 0.20 M tetrabutylammonium hexafluorophosphate as electrolyte, can be used as single-source (unimolecular) precursors to deposit electrochemically Cu–Ni alloy and metal oxide films whose net deposition stoichiometry is controlled by the metal stoichiometry of the precursor.[22] This controlled unimolecular electrodeposition technique may hold the key for producing new types of alloy and mixed-metal oxide films for use in catalysis, microelectronics, magnetic recording media, or other systems in which a well defined atomic-level deposition of metals and metal oxides is required. This process could also lead to new more environmentally benign metal plating technologies.

Part of our research has centred around investigating the electrochemical properties of these complexes in order to understand better the electrochemical mechanisms and optimally to control the alloy and metal oxide film deposition process. In this

---

paper we report on the electrochemical behaviour of the homologous series of the Cu–Ni heteropolymetallic complexes obtained from the transmetallation reaction (1). In addition to the synthesis, physical properties and spectra [15,17,23] for this series of HPM complexes, their thermolytic [24] and electrochemical [22] deposition have also been described.

Experimental

All electrochemical work with the exception of the steady-state voltammetry was conducted with EG&G Princeton Applied Research Models 273 and 263 potentiostat-galvanostats (EG&G, Princeton, NJ) both controlled by a DEC p420sx computer and EG&G M270 electrochemical analysis software. All cyclic voltammetry (CV) experiments were run with iR compensation provided by the M270 software. The steady-state voltammograms were obtained with a Cypress Systems CS-1090 computer controlled electroanalytical system (Cypress Systems, Lawrence, KS).

All experiments were performed with a three-electrode system consisting of a working electrode, platinum counter electrode, and a Ag–AgPF$_6$ (0.01 M)–CH$_3$CN reference electrode, to which all potentials are referenced unless otherwise indicated. Using this reference electrode the peak potential (E_{pa}) for 1 mM ferrocene in dmso–NBu$^t_4$PF$_6$ (0.2 M) was 48 mV. The working electrode for all electrochemical experiments, except the steady-state voltammetry, was a 3 mm diameter (0.071 cm^2) platinum disc (BAS, West Lafayette, IN). The steady-state voltammograms were recorded with a 10 μm diameter platinum disc ultramicroelectrode (Cypress Systems). The working electrodes were polished with 0.05 μM alumina (Buehler), washed with deionized water, sonicated for about 5 min and dried before use. The electrode was routinely tested and considered acceptable for use when the anodic and cathodic peak separation was 70 mV or less at a scan rate of 1 V s^{-1} for 1 mM potassium hexacyanoferrate(III) in 1 M aqueous KCl. Optical microscopic observations of the electrode surfaces were made with a Metaval-H (Leco/Jena) inverted polarizing light microscope. Prior to electrochemical measurements, the solutions were purged for about 10 min and then blanketed with nitrogen gas while the data were collected. All measurements were carried out at room temperature (24 ± 1 °C).

For the electrolysis, the cell consisted of a large mercury-pool working electrode with an area of 15.9 cm^2, a platinum counter electrode, and a Ag–AgPF$_6$ (0.01 M)–CH$_3$CN reference electrode. Samples consisted of 10 or 8 cm^3 aliquots of 1 mM [(μ_4-O)(denc)$_4$Cu$_4$Cl$_6$] or [(μ_4-O)(dmap)$_4$Cu$_4$Cl$_6$] (dmap = 4-dimethylaminopyridine) in dmso with 0.20 M NBu$^t_4$PF$_6$. The solution was stirred and kept under nitrogen during electrolysis.

Electronic spectra were measured with a Cary 1E UV/VIS spectrophotometer in anhydrous dimethyl sulfoxide (Aldrich) or in methylene chloride refluxed over CaH$_2$ and filtered. Room-temperature ^{1}H NMR spectra were measured with a Varian Unity 300 nuclear magnetic resonance spectrometer in (CD$_3$)$_2$SO, CD$_2$Cl$_2$, CDCl$_3$ or CD$_3$CN.

The [(μ_4-O)(denc)$_4$Cu$_4$Cl$_6$] complex used in the transmetallation reaction (1) was synthesized according to the method of Dickenson et al.[8] and the Ni(NS)$_2$ transmetallator according to the procedure of Iskander and El-Sayed.[25] All HPM transmetallation products were made and purified according to previously published procedures.[15,23] The purity of each complex was established with atomic absorption (AA) and other spectroscopic techniques. All the purified Cu–Ni and Ni complexes contained about 5% contamination with unreacted and unseparated Cu$_4$ complex. All experiments were carried out using a 1 mM concentration of the complex in dmso with 0.20 M NBu$^t_4$PF$_6$ as supporting electrolyte. Both the anhydrous dmso and the NBu$^t_4$PF$_6$ were used as received from Aldrich. The cyclic voltammogram of dmso containing 0.20 M NBu$^t_4$PF$_6$ showed a flat background current between 0.3 and −2.4 V.
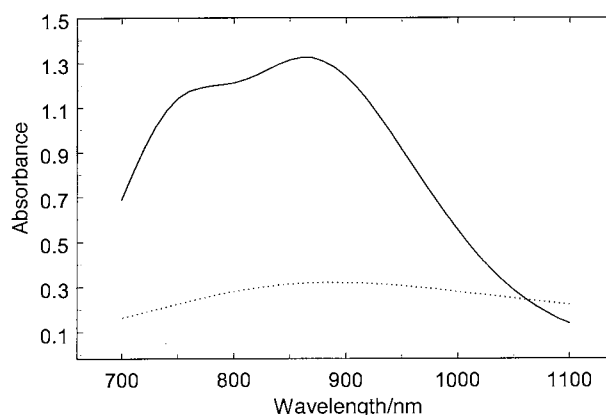

Fig. 1   The electronic spectra of 0.7 mM [(μ_4-O)(denc)$_4$Cu$_4$Cl$_6$] in dmso (- - - -) and methylene chloride (——)

Results and Discussion

Electroactive species in dmso

Preliminary studies showed some differences in the electrochemical behaviour of the complexes in solutions of a co-ordinating solvent such as dmso and a non-co-ordinating solvent such as methylene chloride. The nature of the electroactive species for the five members of the homologous series of copper–nickel complexes [(μ-O)(denc)$_4$Cu$_{4-x}${Ni(H$_2$O)}$_x$Cl$_6$] ($x = 0$–4) in dmso or methylene chloride was addressed with electronic spectroscopy and nuclear magnetic resonance (NMR) measurements.

Fig. 1 shows the electronic spectra obtained using 0.7 mM solutions of [(μ_4-O)(denc)$_4$Cu$_4$Cl$_6$] in dmso and in methylene chloride. For this complex, and all the other members of the series, the two spectral features around 860 and 760 nm for the complexes in CH$_2$Cl$_2$, assigned to the d–d transitions of Cu^{II},[11] are replaced by a single broad maximum centred around 890 nm in dmso. The molar absorptivities at the maxima in dmso decrease with increasing x, similar to the behaviour observed for the complexes in CH$_2$Cl$_2$.[23] Furthermore, stepwise dilutions of concentrated dmso solutions of the complexes with CH$_2$Cl$_2$ show that the 860 and 760 nm spectral features of these complexes can be fully recovered with an approximately 100-fold dilution.

The paramagnetic ^{1}H NMR spectra of the [(μ_4-O)(denc)$_4$Cu$_4$Cl$_6$] complex in dmso showed significant perturbation compared to those observed in the non-co-ordinating solvents CD$_2$Cl$_2$, CDCl$_3$ or CD$_3$CN. For example, in CDCl$_3$ the peaks for H^2 and H^6 on the pyridine ring are at δ 116 and 118, consistent with loss of axial symmetry with substitution in the three position; H^4 is at δ 16.5 and is the same intensity as H^5 at δ 35.8. The ethyl groups of the denc are only slightly perturbed from their positions for the free amide. On the other hand, the spectrum in dmso shows significant perturbation with the proton resonances of the pyridine ring being split. The splitting of the ring protons can be understood in terms of the free rotation of the ring and proximity of the protons relative to the metal centre when dmso co-ordinates to Cu^{II}. There is no evidence of free amide, and the pattern for the ethyl groups is significantly perturbed from that seen in CD$_3$CN or CD$_2$Cl$_2$. There is an increase in the spin relaxation rate, as evidenced by the broadening of the peaks, however the J coupling is essentially unchanged, as evidenced by minor changes in paramagnetic shifts. From the NMR data we feel reasonable in concluding that co-ordination in dmso does not result in ligand loss, but rather in addition of dmso to the co-ordination sphere of Cu^{II}.

Taken together, the UV/VIS and NMR spectroscopic results indicate that dmso solvent molecules act as ligands and increase the co-ordination number of each Cu^{II} centre to six. A change in geometry of the Cu^{II} centres from five-co-ordinate distorted
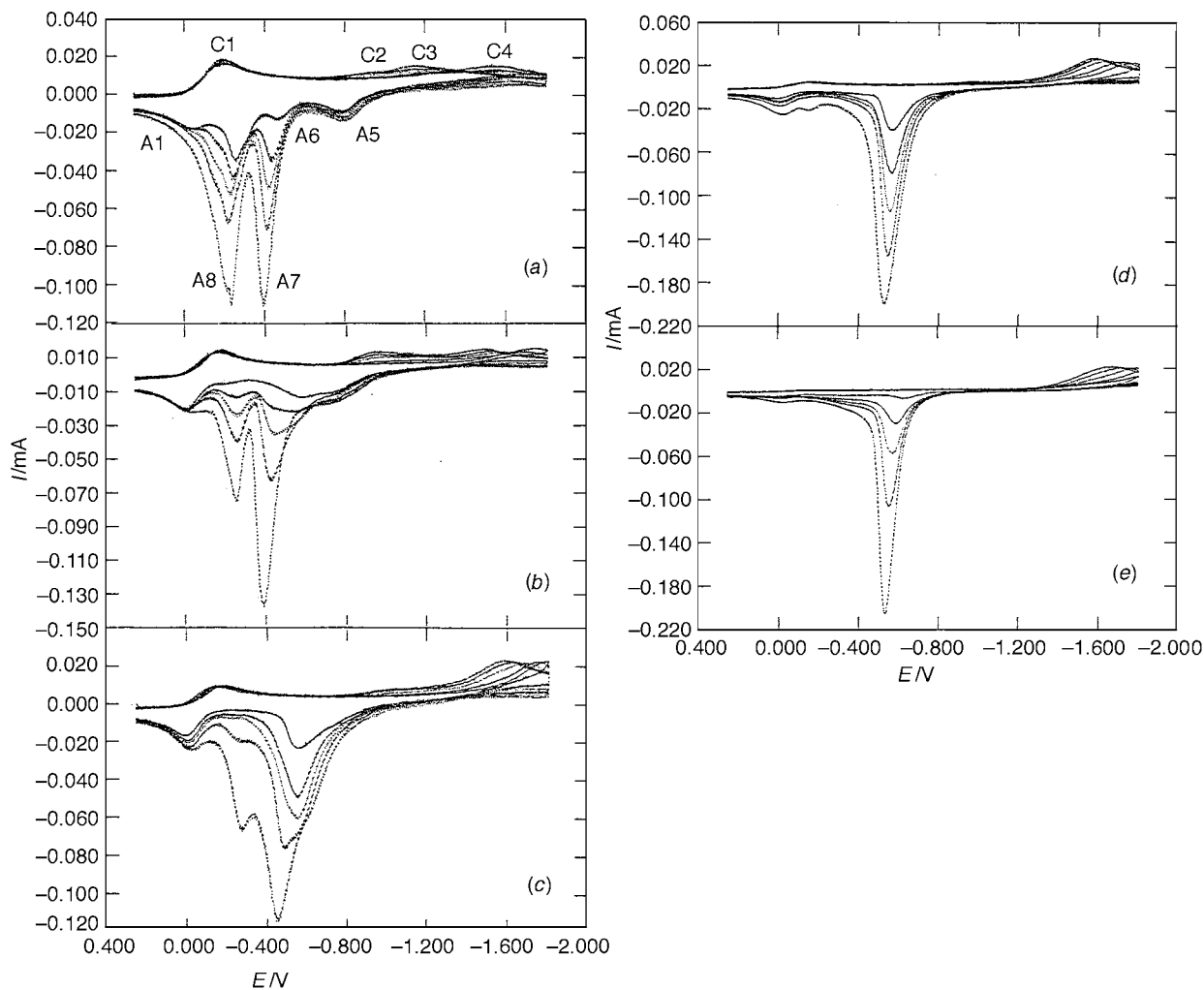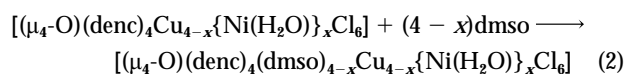
Fig. 2 Cyclic voltammograms at a platinum electrode with 1 mM of the (*a*) Cu_4, (*b*) Cu_3Ni, (*c*) Cu_2Ni_2, (*d*) $CuNi_3$ and (*e*) Ni_4 core complex in dmso–$NBu^t_4PF_6$ (0.02 M), all at a scan rate of 0.05 V s^{-1}. Increasing peak currents correspond with pause times of 0, 10, 20, 40 and 100 s

trigonal bipyramid to six-co-ordinate pseudo-octahedral is consistent with the observed reduction in spectral intensity associated with the d–d transitions of the Cu^{II} centres.[26] Methylene chloride dilutions of dmso solutions of the complexes are consistent with reversible addition of dmso to the co-ordination sphere of the Cu^{II} centres. While it was not possible to identify co-ordinated water in solution it is reasonable to expect that water co-ordinated to the Ni^{II} centres can be replaced with dmso. Most importantly, the absence of free amide for $(CD_3)_2SO$ solutions of the complexes as well as the reversible co-ordination of dmso in CH_2Cl_2–dmso solutions of the complexes support the conclusion that these complexes remain intact and tetranuclear in dmso and contain one dmso molecule per Cu^{II} as the electroactive species according to equation (2).

$$[(\mu_4\text{-}O)(denc)_4Cu_{4-x}\{Ni(H_2O)\}_xCl_6] + (4 - x)dmso \longrightarrow$$
$$[(\mu_4\text{-}O)(denc)_4(dmso)_{4-x}Cu_{4-x}\{Ni(H_2O)\}_xCl_6] \quad (2)$$

General electrochemical behaviour in dmso

Shown in Fig. 2(*a*)–2(*e*) are multiple-scan cyclic voltammograms obtained for the five members of this homologous series of Cu–Ni complexes in the potential range 0.25 to −1.80 V and at a scan rate of 0.05 V s^{-1}. Each scan was paused at the switching potential for 0, 10, 20, 40 and 100s. The first scan was taken after cleaning and polishing the electrode while the rest of the scans are continuous. The anodic and cathodic potential limits of 0.25 and −1.80 V, respectively, were necessitated by two processes occurring past these points. If the starting potential is

more anodic than about 0.25 V, an initial oxidation current is observed and subsequent peaks during the scan become increasingly irreproducible, most likely due to an oxidation product adsorbed on the electrode surface. The cathodic limit occurs due to the reduction of the supporting electrolyte at potentials greater than −2.4 V and to the bulk electrodeposition of the metals from the complex (deposition of even a very thin Cu–Ni film affects the reproducibility of the electrode and its effects can only be reversed by polishing).

This series of cyclic voltammograms (Fig. 2) dramatically demonstrates the changes caused by the sequential substitution of Cu by Ni in the Cu_4 core complex. Two significant changes are observed as the number of Ni atoms in the core increases. *First*, there is a systematic decrease and disappearance of the redox couple centred at about −0.1 V (C1, A1). As will be shown later, this couple is due to solution electrochemistry and results from the reduction of Cu^{II} to stable Cu^{I} centres within the complex. *Secondly*, the anodic peaks between −0.2 and −0.4 V (A7, A8) disappear and a new single narrow peak (A6) appears at −0.6 V, proportional to the increase in the number of Ni centres.

The formation of a deposit on the electrode surface during the CV is readily visible in the voltammogram for each complex. For the Cu_4 and Cu_3Ni complexes, two anodic peaks [A8, A7; Fig. 2(*a*) and 2(*b*)] predominate and both linearly increase with pause time. A parallel situation is also observed for the Ni_4 and $CuNi_3$ complexes but with only a single anodic peak [A6; Fig. 2(*d*) and 2(*e*)]. As might be expected, the Cu_2Ni_2 complex shows the most complicated 'mixed' behaviour, but the collection of peaks between A8 and A5 [Fig. 2(*c*)] are intermediate.
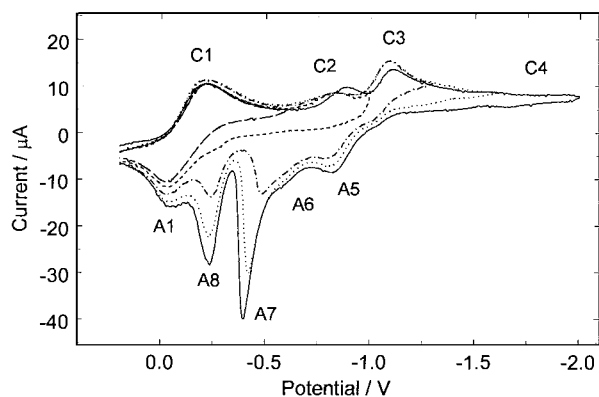
Fig. 3 The effect of switching potential on the anodic sweep for the CV of a 1 mM solution of $[(\mu_4\text{-O})(\text{denc})_4\text{Cu}_4\text{Cl}_6]$ in dmso–NBu$^\text{t}_4$NPF$_6$ (0.20 M) with $v = 0.02$ V s^{-1}

Fig. 4 Cyclic voltammograms at a platinum electrode for 1 mM solutions of the (a) Cu$_4$, (b) Cu$_3$Ni, (c) Cu$_2$Ni$_2$, (d) CuNi$_3$ and (e) Ni$_4$ core complexes in dmso–NBu$^\text{t}_4$PF$_6$ (0.02 M) with $v = 0.05$ V s^{-1}

Several of the other cathodic and anodic peaks also show some very slight changes, most likely due to some residual deposit remaining on the electrode surface after each scan.

Owing to the complexity seen in the voltammograms above, the redox electrochemistry was further investigated by varying the switching potential. Shown in Fig. 3 are the superimposed cyclic voltammograms for the Cu$_4$ complex recorded after switching the potential at -0.6, -1.0, -1.3, -1.6 and -2.0 V. The resulting voltammograms become increasingly more complex, with multiple anodic and cathodic peaks appearing at the more cathodic switching potentials. Switching at -0.6 V produces a simple and easily reproducible redox couple whose peak heights decrease in proportion to the number of Cu atoms in the complex. Switching just past the second cathodic peak at -1.0 V (C2) does not result in a corresponding anodic peak, indicating both the lack of deposition and reversible electrochemical behaviour. Peak C2 does not increase with scan rate and thus may be the result of an adsorbed species. Switching at a potential $\geqslant -1.3$ V, slightly cathodic of C3, results in the appearance of three anodic peaks (A5, A7, A8) which increase proportionally to the amount of time spent cathodic of C3 [see Fig. 2(a)].

Solution electrochemistry

Owing to the difficulties involved in studying such complicated electrodeposition processes as these, we limited our preliminary investigations mainly to the initial steps of the reduction processes for the redox couple shown in Fig. 2 (C1, A1). As before, the initial and switching potentials where chosen to eliminate, to the maximum extent possible, any interferences from the adsorption of oxidation products at the anodic end and the formation of Cu–Ni films at the cathodic end. Repetitive cycling between 0.25 and -0.45 V showed no difference between the first and fifteenth scan for any of the complexes. This indicates that coverage of the electrode surface with adsorbed oxidation products and/or electrodeposited metals did not occur and the CV redox couple is due entirely to solution electrochemistry.

A typical example of the cyclic voltammograms obtained for each complex in the potential range of 0.25 to -0.45 V at a scan rate of 0.05 V s^{-1} is shown in Fig. 4. The dependence of the cathodic peak current (i_{pc}) and peak potential (E_{pc}) on the Cu–Ni stoichiometry of the complexes is graphically shown in Fig. 5(a) and 5(b), respectively. In general, both i_{pa} and i_{pc} decrease linearly in proportion to the decrease in the number of Cu atoms. However, i_{pa} for a given complex is not as reproducible and is probably more easily perturbed by the adsorption process occurring at the switching potential. The cyclic voltammogram for the Ni$_4$ complex shows a small peak which is due to contamination by unreacted and unseparated Cu$_4$ complex remaining from the synthesis (about 5%). Several attempts to
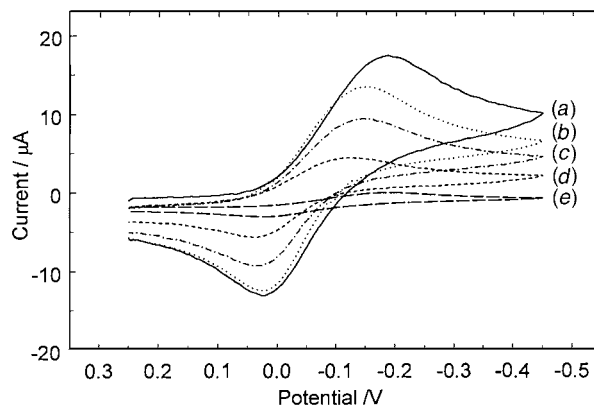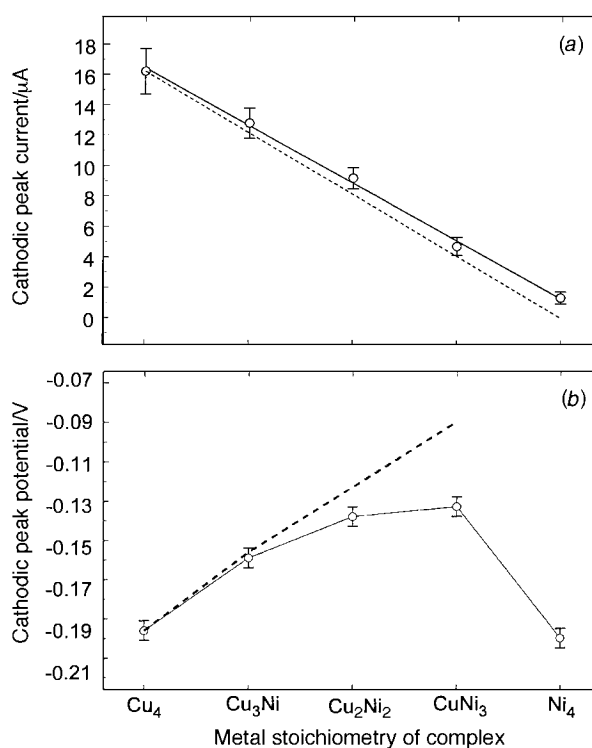

Fig. 5 Plot of the cyclic voltammographic (a) cathodic peak current (i_{pc}) and (b) peak potential, as a function of the metal stoichiometry of the complex $[(\mu_4\text{-O})(\text{denc})\text{Cu}_{4-x}\{\text{Ni}(\text{H}_2\text{O})\}_x\text{Cl}_6]$ ($x = 0$–4) and indicating assumed response when corrected for Cu$_4$ contamination (- - - -)

eliminate the Cu$_4$ complex residue were unsuccessful. Its presence was independently confirmed in all complexes by AA, X-ray diffraction (XRD) and X-ray photoemission spectroscopy (ESCA).[22]

The anodic and cathodic peak potentials (E_{pa} and E_{pc}) both independently exhibit an apparent non-linear relationship with the number of Ni atoms. Both peaks shift to more anodic potentials and become broader and closer together as the number of Ni atoms increases. This apparent non-linear behaviour is most likely due to the Cu$_4$ complex contamination which represents an increasing fraction of the Cu species in the samples and which we suspect is responsible for both slightly broadening and *cathodically* shifting the CV peaks. The contamination represents only about 7% of the total Cu$^\text{II}$ in the Cu$_3$Ni complex sample and thus has very little effect on the CV peak potential in this case. However, it represents 10% of the Cu$_2$Ni$_2$ contamination and 17% of the CuNi$_3$ contamination. The CV peak seen for the Ni$_4$ complex is due entirely to the Cu$_4$ contamination. If we adjust the shift of the peak potential in

Table 1 Number of electrons and diffusion coefficients as determined by two different methods for each complex

| Complex | Method A | | Method B | | Average |
	n	$10^6 D/$ cm^2 s^{-1}	n	$10^6 D/$ cm^2 s^{-1}	n
Cu$_4$	3.1 ± 0.2	1.9(±0.2)	3.1 ± 0.2	2.2(±0.1)	3.1 ± 0.1
Cu$_3$Ni	2.0 ± 0.2	2.4(±0.3)	2.1 ± 0.1 *	2.2(±0.1)	2.1 ± 0.2
Cu$_2$Ni$_2$	2.0 ± 0.2	1.7(±0.2)	1.7 ± 0.1 *	2.2(±0.1)	1.8 ± 0.2
CuNi$_3$	0.62 ± 0.1	1.5(±0.3)	0.52 ± 0.1 *	2.2(±0.1)	0.57 ± 0.12

* Recalculated from Method A data.

proportion to the contamination (*i.e.* 7, 10, 17 and 100% more anodic from the Cu$_4$ potential), the peak potentials present a more linear relationship with increasing Ni content as shown in Fig. 5(*b*). From this anodic shift one may infer that it becomes slightly easier to transfer electrons as the Cu^{II} is replaced by Ni^{II} in the core structure.

The peak separation (ΔE_p) of the redox couple between 0 and -200 mV (Fig. 2, peaks C1, A1 and Fig. 4) for each complex was also studied as a function of the CV sweep rate (ν). This redox couple for all Cu–Ni complexes displayed the diagnostic criteria expected of a quasi-reversible charge-transfer system. On the Pt electrode, for $\nu = 0.01$–20 V s^{-1} the ΔE_p separation varied linearly from 120 to 800 mV, with the current function $i_p/\nu^{\frac{1}{2}}$ being constant and independent of ν, with peak broadening and the ratio $i_{pa}/i_{pc} \approx 1$. Recent preliminary studies (to be published in a separate paper) indicate that the CV of this couple, at a hanging mercury drop electrode, is reversible with $\Delta E_p = 60$ mV and a consecutive three-electron transfer.

Determination of the number of electrons transferred and the diffusion coefficients

The CV results obtained above appear to indicate that electron transfer initially occurs only to the Cu^{II} centres and that the electron-transfer reaction appears to be quasi-reversible. Further data for the Cu^{II} core reduction processes and the electrochemical reaction can be obtained by determining the number of electrons transferred (n) and the diffusion coefficients (D). Two independent electrochemical techniques were employed to determine n and D for all the complexes in the potential range 0.250 to -0.450 V.

First, we used both steady-state voltammetry at a ultramicroelectrode and chronoamperometry at a microelectrode to determine n and D simultaneously for all complexes.[27] This was accomplished by simultaneously solving the two relationships (3) and (4) giving the slope (S) of the chronoamperometric i *vs.*

$$S = (nFAC\sqrt{D})/\sqrt{\pi} \qquad (3)$$

$$i_{ss} = 4rnFCD \qquad (4)$$

$t^{-\frac{1}{2}}$ plot and the limiting steady-state current (i_{ss}) at a microelectrode, respectively, where r is the radius of the microdisc electrode, A is the area of the microelectrode, and all other symbols have their usual meaning. In the chronoamperometric experiments, the potential was stepped from a value where there was no Faradaic current (about 0.1 V) to a potential of -0.4 V, which is about 200 mV more cathodic than the first reduction peaks of all the complexes. The electrochemically active area of the 3 mm diameter Pt disc electrode was determined from the slope of the chronoamperometric i *vs.* $t^{-\frac{1}{2}}$ plot obtained with 10.4 mM of ferrocene in 0.10 M NEt$_4$ClO$_4$–dmso and was found to be 0.079 ± 0.004 cm^2. The value of D for ferrocene used in calculating this area was 5.4(±0.1) × 10^{-6} cm^2 s^{-1} and was obtained from the limiting current of the steady-state voltammogram using the geometric size of the 10 μm diameter
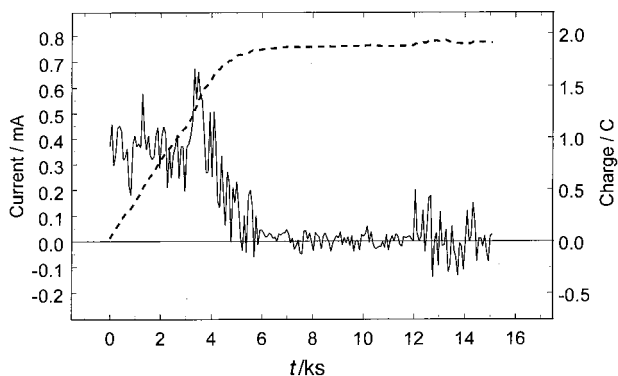

Fig. 6 The chronoamperometric (——) and chronocoulometric (----) response for exhaustive electrolysis of 8 cm^3 of 1 mM [(μ$_4$-O)-(denc)$_4$Cu$_4$Cl$_6$] in dmso–NBu$^t_4$PF$_6$ (0.20 M) at a large mercury-pool working electrode with a Pt counter electrode and a Ag–AgPF$_6$ (0.01 M)–CH$_3$CN reference electrode. Solution was stirred and kept under N$_2$ during electrolysis
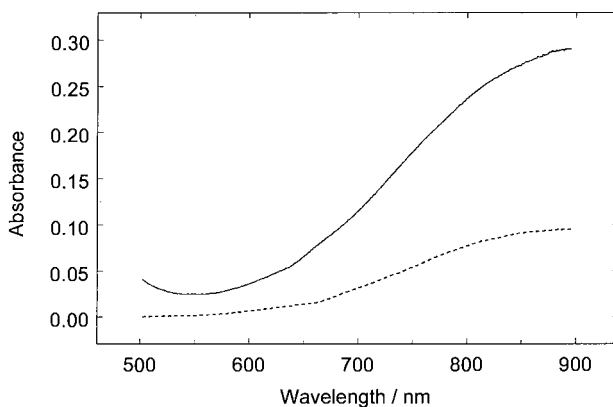

Fig. 7 The electronic spectrum for the d–d transition of Cu^{II} in the complex for the electrolysis shown in Fig. 6 taken at $t = 0$ (——) and 14.4 ks (----)

Pt microdisc electrode and equation (4). The value of n of the ferrocene–ferrocenium couple was taken to be 1. The average of three experimentally determined values of n and D are shown in Table 1, Method A.

In a recent study of ligand effects on the [(μ$_4$-O)L$_4$Cu$_4$Cl$_6$] complexes,[28] we determined n and D by exhaustive electrolysis (chronoamperometry) and spectroscopic monitoring of the electrolysis products. The results for the [(μ$_4$-O)(denc)$_4$Cu$_4$Cl$_6$] complex are of particular interest for this study and were thus supplemented by several additional replications which are presented here in brief summary. Fig. 6 shows a typical example of the chronoamperometric and chronocoulometric response obtained during the exhaustive electrolysis. The average values calculated from five replicate samples were $n = 3.1 \pm 0.1$ and $D = (2.2 \pm 0.1) \times 10^{-6}$ cm^2 s^{-1}. The noise recorded during the electrolysis and over extensive periods (generated most likely by the stirring) was random, appearing at different time intervals for all samples studied with no significant effect on the overall measured charge. The most interesting aspect of this experiment is revealed when we combine the results of the exhaustive electrolysis with those of the accompanying spectroscopic analysis of the products. Fig. 7 shows the electronic spectrum for the d–d transition of Cu^{II} in the complex taken before and after ≈4 h of exhaustive electrolysis. The average of two measurements gives an absorbance of 0.29 before and 0.080 after electrolysis. This indicates that 27% of the copper atoms are still in the Cu^{II} form. Since the electrolysis appears complete we can reasonably assume that these Cu^{II} atoms reside as single centres in the [(μ$_4$-O)(denc)$_4$Cu^{II}Cu$^I_3$Cl$_6$] complex.

To improve the reliability of n and D further, we then used the average value of D determined from the above exhaustive

Table 2 Number of electrons that can be transferred per complex face and the apparent total number predicted (n')

Core structure	Face 1	Face 2	Face 3	Face 4	n'
Cu_4	$3e^-$	$3e^-$	$3e^-$	$3e^-$	3.00
Cu_3Ni	$3e^-$	$2e^-$	$2e^-$	$2e^-$	2.25
Cu_2Ni_2	$2e^-$	$2e^-$	$1e^-$	$1e^-$	1.50
$CuNi_3$	$1e^-$	$1e^-$	$1e^-$	$0e^-$	0.75

electrolysis, and relationships (3) and (4), to recalculate n for the other complexes from the chronoamperometric and voltammetric data. This procedure assumes that D will be approximately the same for all Cu–Ni complexes. This is probably true since the substitution of $Ni(H_2O)$ for $Cu(L)$ in such a large molecule as $[(\mu_4\text{-}O)(denc)_4Cu_4Cl_6]$ should have negligible effect on the diffusion constant. The recalculated values of n are shown in Table 1, Method B.

The number of electrons determined above for this initial redox couple varies roughly from $n = 3$ for the Cu_4 complex to $n = 0.6$ for the $CuNi_3$ complex. Since only a single CV peak results for all of the complexes (Fig. 2, peak C1, A1), the electron transfer is either simultaneous or consecutive with closely spaced $E°$ potentials. A simultaneous three-electron transfer process seems unlikely[29,30] and should produce a much sharper CV peak. On the other hand, our attempts to isolate individual one-electron steps at fast sweep rates up to 150 V s^{-1} as suggested by Pierce and Geiger[31] or by using differential pulse voltammetry did not resolve this question either. The most reasonable assumption is that we have a consecutive transfer of three electrons with the same or closely spaced $E°$. This assumption has also been borne out by a reasonable fit of the experimental CV data with a simulated cyclic voltammogram using three electrons with very closely spaced $E°$ potentials.

Proposed model for heterogeneous electron transfer

As shown in Table 1 and Fig. 4, the addition of electrons to the $Cu_{4-x}Ni_{4x}$ core gives a CV redox couple (C1, A1) for which i_p and n appear to correlate with the replacement of the Cu by Ni. If we assume that electron transfer takes place through the ligands directly to the Cu_4 centres, then we should expect to see $n = 4$ decrease stepwise to $n = 1$ as we replace each Cu by a Ni. However, as Table 1 clearly shows, this is not the case. To explain why all of the Cu^{II} centres in $[(\mu_4\text{-}O)(denc)_4Cu_4Cl_6]$ are not reduced, and to account for the non-integer decrease of n with increasing Ni content, we propose that electron transfer does not occur through the ligands but instead may take place through three of the bridging chlorines on one 'face' of the complex. In addition, once the three electrons are transferred (for the Cu_4 complex), the energetics may not allow transfer of the fourth electron at that point or at a later approach.

The number of electrons that can be transferred to each $[(\mu_4\text{-}O)(denc)_4Cu_{4-x}\{Ni(H_2O)\}_xCl_6]$ species to effect a reduction can be determined by invoking a 'statistically-based' heterogeneous reduction mechanism. In general, the complexes diffuse towards the electrode surface with random orientations. However, one can assume a mechanism such that only one orientation of the complex with respect to the electrode will allow electron transfer to occur. Thus, the complex must bring a core face (*i.e.* three, two-co-ordinate Cl atoms, one on each edge of $Cu_{3-x}Ni_x$ face) in close proximity of the surface. This can be easily accomplished since the ligands do not require much energy to be pushed back. For the Cu_4 complex, the Cl atoms can then bridge the transfer of one electron to each Cu^{II} centre in a face to create the same number of Cu^I centres in that face. The maximum of $n = 3$ implies that the $[(\mu_4\text{-}O)(denc)_4Cu^{II}\text{-}Cu^I_3Cl_6]$ complex cannot accept a fourth electron at applied potentials of less than -1.0 V. This explanation is in accord

with the exhaustive electrolysis experiment described above but does not rule out the statistical argument that there is a certain probability that the reduced complex will return to the surface for another electron transfer with a given face. This model also assumes that there is no electron exchange between mixed oxidation state Cu^I/Cu^{II} centres to effect an internal redox. A ferromagnetic exchange interaction is known for the $[(\mu_4\text{-}O)\text{-}(denc)_4Cu^{II}_{4-x}\{Ni^{II}(H_2O)\}_xCl_6]$ complexes, based on their solid-state magnetic behaviour. The extent of exchange interaction between metal centres for the complexes in dmso, as well as for the Cu^I/Cu^{II} mixed-oxidation-state species is the subject of a future investigation.

For the other $Cu_{3-x}Ni_x$ complexes the observed number of electrons transferred depends on the probability of each face transferring an electron. Table 2 shows the number of electrons transferred for each face of each $Cu_{3-x}Ni_x$ complex and the predicted value n' based on this model. It is clear in comparing the last columns of Tables 1 and 2 and the peak current data in Fig. 5 that there is excellent agreement between n and n' for all the complexes.

Conclusion

From the above results it appears reasonable to conclude that the first cathodic peak (C1) in the cyclic voltammogram of the Cu-containing complexes (Figs. 2, 3 and 4) is due to the reduction of one, two or three of the Cu^{II} centres to Cu^I and that this process occurs by consecutive electron transfers. The number of electrons transferred in this potential region, based on the CV studies, depends on the metal composition of the complexes with $n = 3.1$, 2.1, 1.8 and 0.57 for the Cu_4, Cu_3Ni, Cu_2Ni_2 and $CuNi_3$ complexes, respectively. The model proposed for the electron-transfer mechanism gives values of n in very good agreement with the observed data and accounts for both the electrochemical and spectroscopic observations. It also appears that for all four Cu complexes the electron transfer is chemically reversible and that the Cu^I-containing complex is stable within the time-frame of the experiments described here. As the potential is scanned to more cathodic potentials, the remaining Cu^I and Cu^{II} centres are reduced at around -1.0 V and eventually the Ni^{II} centres are reduced at about -2.0 V. As reported in previous work,[22] for the deposits made between -2.0 to -2.2 V, both XRD and ESCA investigations of the electrode surface have conclusively shown that this deposited hard metallic-like film consists mainly of Cu^0–Ni^0 alloy, Cu_2O, NiO and $Ni(OH)_2$, with the proportions varying with the metal content of the complex. From this data and from results of the partial anodic scans (Fig. 3), the three anodic peaks (A6, A7 and A8) in Fig. 2 can be assigned to the reoxidation of the deposited material *via* Cu^0–$Ni^0 \longrightarrow Cu^{II} + Ni^{II}$, $Cu_2O \longrightarrow Cu^{II}$ and $Cu^0 \longrightarrow Cu^{II}$, respectively.

The electrochemistry of these heteropolymetallic complexes is unique in that the electron transfers appear to be consecutive and at about the same potential (on a Pt electrode) and may even be electrochemically reversible and consecutive on a mercury electrode. Further studies are needed to examine the number of electrons transferred using exhaustive electrolysis for the Cu_3Ni, Cu_2Ni_2 and $CuNi_3$ complexes. Total electrolysis of these complexes with a resulting $n = 3.0$, 2.0 and 1.0, respectively, would put in doubt the orientation hypothesis while $n = 2.25$, 1.50 and 0.75 would certainly lend weight to some sort of orientation or adsorption driven reaction. We are also planning to look at the kinetic and ligand effects for the Cu–Ni family and also compare the Cu–Ni behaviour with other metal complexes such as Co–Cu and Co–Ni.

Acknowledgements

References

1 J. A. Bertrand and J. A. Kelley, *J. Am. Chem. Soc.*, 1966, **88**, 4746.

2 J. A. Bertrand, *Inorg. Chem.*, 1967, **6**, 495.

3 C. M. Harris and E. Sinn, *Inorg. Nucl. Chem. Lett.*, 1969, **5**, 125.

4 B. T. Kilbourne and J. D. Dunitz, *Inorg. Chim. Acta*, 1967, **1**, 209.

5 B. D. Bright and J. N. Helle, *Acta. Crystallogr., Sect. B*, 1972, **28**, 3436.

6 M. R. Churchill and B. G. DeBoer, *Inorg. Chem.*, 1975, **14**, 2502.

7 H. M. Haendler, *Acta. Crystallogr., Sect. C*, 1990, **46**, 2054.

8 R. C. Dickenson, F. T. Helm, W. A. Baker, T. D. Black and W. H. Watson, *Inorg. Chem.*, 1977, **16**, 1530.

9 F. J. Keij, J. G. Haasnoot, A. J. Oosterling, J. Reedijk, C. J. O'Connor, J. H. Zhang and A. L. Spek, *Inorg. Chim. Acta*, 1991, **181**, 185.

10 M. A. Sayed, A. Ali, G. Davies, S. Larsen and J. Zubieta, *Inorg. Chim. Acta*, 1992, **194**, 139.

11 H. tom Dieck, *Inorg. Chim. Acta*, 1973, **7**, 397.

12 H. L. Felderova, D. Makanova and G. Dersi, *J. Therm. Anal.*, 1991, **37**, 2335.

13 G. Davies, M. A. El-Sayed and A. El-Toukhy, *Chem. Soc. Rev.*, 1992, **21**, 101.

14 K. G. Caulton, G. Davies and E. M. Holt, *Polyhedron*, 1990, **9**, 2319.

15 A. El-Toukhy, G. Z. Cai, G. Davies, T. Gilbert, K. Onan and M. Veidis, *J. Am. Chem. Soc.*, 1984, **106**, 4596.

16 S. Al-Shehri, G. Davies, M. A. El-Sayed and A. El-Toukhy, *Inorg. Chem.*, 1990, **29**, 1198.

17 A. Abu-Raqabah, G. Davies, M. El-Sayed and A. El-Toukhy, *Inorg. Chem.*, 1989, **28**, 1156.

18 G. Davies, M. A. El-Sayed, A. El-Toukhy, M. Henary and T. R. Gilbert, *Inorg. Chem.*, 1986, **25**, 2373.

19 M. A. El-Sayed, A. El-Toukhy, K. Z. Ismael and A. A. El-Maradne, *Inorg. Chim. Acta*, 1991, **182**, 213.

20 S. P. Kounaves, B. Workie, A. Robbat and G. Davies, *Electrochemical Society, 184th Meeting Extended Abstracts*, 1993, vol. 93-2, Abstract 565.

21 C. Dubé, S. P. Kounaves, A. Robbat and B. Workie, *Electrochemical Society, 185th Meeting Extended Abstracts*, 1994, vol. 94-1, Abstract 918.

22 C. E. Dubé, B. Workie, S. P. Kounaves, A. Robbat, M. L. Aksu and G. Davies, *J. Electrochem. Soc.*, 1995, **142**, 3357.

23 G. Davies, M. A. El-Sayed and A. El-Toukhy, *Inorg. Chem.*, 1986, **25**, 2269.

24 G. Davies, B. C. Giessen and H.-L. Shao, *Mater. Lett.*, 1990, **9**, 231.

25 M. E. Iskander and L. El-Sayed, *Inorg. Nucl. Chem.*, 1971, **33**, 4253.

26 A. B. P. Lever, *Inorganic Electronic Spectroscopy*, Elsevier, Amsterdam, 1984.

27 A. S. Baranski, W. R. Fawcett and C. M. Gilbert, *Anal. Chem.*, 1985, **57**, 166.

28 M. L. Aksu, B. Workie, S. P. Kounaves, A. Robbat, C. E. Dubé and G. Davies, unpublished work.

29 A. Pross, *Acc. Chem. Res.*, 1985, **18**, 212.

30 S. Efirma, *Isr. J. Chem.*, 1985, **22**, 401.

31 D. T. Pierce and W. E. Geiger, *J. Am. Chem. Soc.*, 1989, **111**, 7636.